Journal of Molecular Structure 1206 (2020) 127661

Contents lists available at ScienceDirect

Journal of Molecular Structure

journal homepage: http://www.elsevier.com/locate/molstruc

Structure activity relationship analysis of antiproliferative cyclic C_5-curcuminoids without DNA binding: Design, synthesis, lipophilicity and biological activity

Imre Huber [a, *], Zsuzsanna Rozmer [a], Zoltán Gyöngyi [b], Ferenc Budán [b], Péter Horváth [c], Eszter Kiss [c], Pál Perjési [a]

[a] Department of Pharmaceutical Chemistry, University of Pécs, Pécs, H-7624, Hungary
[b] Department of Public Health Medicine, Medical School, University of Pécs, Pécs, H-7624, Hungary
[c] Department of Pharmaceutical Chemistry, Semmelweis University, Budapest, H-1092, Hungary

ARTICLE INFO

Article history:
Received 31 October 2019
Accepted 26 December 2019
Available online 9 January 2020

Keywords:
Cyclic C_5-curcuminoids
Cytotoxic
Experimental log*P*
SAR
DNA binding
Antiproliferative

ABSTRACT

The chemical susceptibility of the β-diketone linker between the two aromatic rings in the structure of curcumin to hydrolysis and metabolism has made it crucial to investigate structurally modified analogs of curcumin without such shortcomings. The synthesis of twenty cyclic C_5-curcuminoids is described in this study in order to gain more insight into their anticancer structure-activity relationship (SAR). The design of their synthesis included four different cyclanones and five substituted aromatic aldehydes to form four, five-membered subgroups. These model compounds were evaluated *in vitro* for antiproliferative activity in an XTT cell viability assay against MCF-7 human non-invasive breast adenocarcinoma cancer cells and Jurkat human T lymphocyte leukemia cells in five different concentrations (10 nM, 100 nM, 1 μM, 10 μM and 20 μM). The majority of the compounds investigated have shown remarkable cytotoxicity with IC_{50} values in the range of 120 nM and 2 μM with very high relative toxicity values to curcumin. The SAR conclusions are drawn and summarized. A method was developed and applied in a TLC based experimental log*P* measurement, which is new for such C_5-curcuminoids. The log*P* data and structural modifications have shown a strong correlation. The correlation of these experimental log*P* and the corresponding IC_{50} values of the model-compounds were calculated according to the Pearson and Kendall correlation coefficient and showed weak concordance. The physicochemical behaviors of the majority of these compounds are in good accordance with Lipinski's rule. The most promising compound is **7a**, which is the most active (IC_{50} = 0.12−0.32 μM), most potent (80 times of curcumin) with the lowest lipophilicity (experimental log*P* = 3.22) which is important also from a pharmacokinetic point of view. The analysis of experimental log*P* and computed Clog*P* values have revealed good agreement. These cyclic C_5-curcuminoids in contrast to curcumin do not bind to natural DNA based on their CD spectra.

1. Introduction

Plants are unbeatable sources of nutraceuticals. They are also considered to be one of the major sources of lead molecules and drug candidates [1]. The intense yellow rhizome of herbs in the *Zingiberaceae* (ginger) family provides turmeric. Species like *Curcuma longa* L. and/or *Curcuma domestica* L. for example, are used to prepare that well-known spice nowadays. The major component of turmeric is its secondary metabolite, curcumin (Fig. 1). The preventive and therapeutic applications of curcumin are extremely diverse. Many clinical trials have been conducted to evaluate their pharmacokinetics, safety and efficacy. In cancer, cardiovascular diseases, diabetes, inflammatory diseases and communicable diseases, chronic arsenic exposure and alcohol intoxication, curcumin has been analyzed [2].

Extensive research has shown that curcumin exhibits many different pharmacological effects and has a number of molecular targets with multiple pathways as an antiproliferative molecule [3,4]. Curcumin (diferuloylmethane), 1,7-bis(4-hydroxy-3-

* Corresponding author.
E-mail address: imre.huber@aok.pte.hu (I. Huber).

https://doi.org/10.1016/j.molstruc.2019.127661

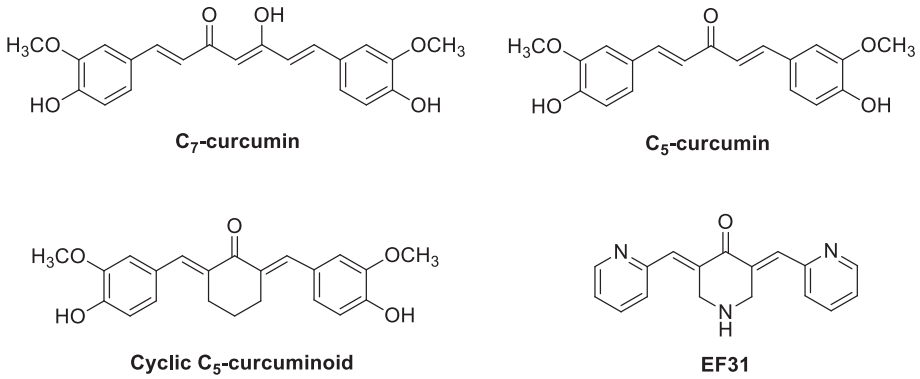

Fig. 1. Natural curcumins and synthetic homocyclic or heterocyclic C_5-curcuminoids.

methoxyphenyl)-1,6-heptadien-3,5-dion has a *ß*-diendione linkage (1,6-heptadien-3,5-dion) containing seven carbon atoms (C_7) between the two arylidene groups in its structure (Fig. 1). It was a belief for a long time, that natural curcuminoids (including the metabolites of curcumin) are exclusively C_7-curcuminoids. However, along with curcumin, a C_5-curcuminoid was also isolated from both *Curcuma longa* and *Curcuma domestica* [5,6]. This natural C_5-curcumin [7], 1,5-bis(4-hydroxy-3-methoxyphenyl)-1,4-pentadiene-3-one, as a truncated analog of curcumin contains a C_5 *ß*-dienone linker (1,4-pentadiene-3-one) between the two benzylidene cores in its structure (Fig. 1).

This compound, C_5-curcumin and its related derivatives proved to be more potent anticancer molecules compared to curcumin [7,8]. Their interesting reversible *thia*-Michael reaction, which is principal in binding to the biological place of action of such curcuminoids is described in detail [8].

In view of the discovery of C_5-curcumin showing superior anticancer activity to curcumin, a number of new cyclic C_5-curcuminoids have been synthesized. Structural modifications of C_5-curcuminoids focusing on enhancing their bioactivities have been investigated intensively during the last couple of decades. Curcumin, C_5-curcumin and cyclic C_5-curcuminoids were subjected to structure-activity relationship (SAR) studies [3,6–9] in order to find details on the most appropriate structural changes for the best cytotoxic effect.

The synthetic, cyclic C_5-curcuminoid with a cyclohexanone core (Fig. 1) for example proved to be more active against castration-resistant prostate cancer compared to curcumin both *in vitro* and *in vivo* [9]. Numerous studies have been conducted also on the (3*E*,5*E*)-3,5-dibenzylidene-4-piperidone synthetic, heterocyclic C_5-curcuminoid family [10–15]. It became clear about these 4-piperidone derivatives that they exhibit higher cytotoxicity than curcumin towards different tumor cell lines like breast, prostate, cervix, melanoma, etc. [3]. Compound **EF31** for example (Fig. 1), similarly to related derivatives is shown to be a pleiotropic inhibitor of kinases (relevant to many forms of cancer), that operate at multiple points along cell signaling pathways. In addition to superior cytotoxicity to curcumin, these 4-piperidone derivatives show differential cytotoxicity; they are less toxic to non-cancer cells when compared to cancer cells [10,13,16,17].

Another crucial advantage of these synthetic C_5-curcuminoids is that a number of them are able to revert multi-drug resistance (MDR) [14,16,17]. Moreover, there are reports on the *in vivo* tolerability and lack of acute toxicity of these curcuminoids on rodents [18]. A number of C_5-curcuminoids have several different modes of action, such as inducing apoptosis, cell cycle arrest, inhibiting the biosynthesis of polypeptides fundamental to tumor-progression, affecting mitochondrial respiration and stimulation/inhibition of certain enzymes playing a role in tumor growth [19].

These cyclic C_5-curcuminoids bear a β-dienon cross-conjugated moiety essential for cytotoxicity [22] in their structure. This β-dienon function is a reactive and selective Michael-acceptor [8]. Selectivity appears in the fact that the Michael-reaction takes place exclusively with the nucleophilic thiol groups of biological macromolecules. It seems to be logical, that these curcuminoids cannot react with DNA in contrast to curcumin [20,21]. To gain details and proof of their mode of action in this respect we decided to perform CD spectroscopic investigations. Such CD spectroscopic data about the cyclic and heterocyclic C_5-curcuminoids are not available in the corresponding literature to our knowledge. In view of the considerations above as a continuation of our previous SAR studies [22,23], and to gain more insight into the influence of structural modifications on the cytotoxic activity of such homocyclic and heterocyclic C_5-curcuminoids we resynthesized twenty previously described molecules (see experimental part) for a systematic SAR study. These C_5-curcuminoids are less susceptible to metabolism compared to curcumin [24,25]. We selected the following two cell-lines to perform XTT cell viability assays: MCF-7 (human non-invasive breast cancer cells) and Jurkat (human T lymphocyte leukemia cells). We applied an RP-TLC method to measure the experimental log*P* values of the twenty selected molecules. Some physicochemical parameters of the molecules were also computed in order to obtain the corresponding calculated Clog*P* values for example.

2. Experimental

2.1. Chemical synthesis

For the synthesis of the model compounds of this study, we have used a previously described “one pot” method of ours [22]. These compounds are known from the chemical literature and were prepared according to known methods, like **6a** [38], **6b**, **6c**, **6d** [39], **6e** [40], **7a**, **7d**, **7e** [41], **8a**, **8d** [42] and **8e** [43]. We have recorded their ^{1}H NMR spectra and measured their melting points. Our own physical data are in good accordance with the published parameters. Chemicals, solvents and reagents for the study were purchased from Alfa Aesar, Molar and Merck Ltd (Budapest, Hungary). Melting points were determined on a Barnstead-Electrothermal 9100 apparatus and are uncorrected. Silica gel 60 (0.2–0.5 mm, MERCK) was used for column chromatography and pre-coated silica gel 60 (F-254, MERCK) plates for TLC.

NMR: ^{1}H NMR spectra were obtained using a Varian UNITY INOVA 400 WB spectrometer. Chemical shifts are referenced to the residual solvent signal. Measurements were run at a probe temperature of 298 K in $CDCl_3$ or DMSO-d_6 solutions. All the ^{1}H NMR

spectra were in accordance with the expected structures.

2.2. CD

CD and UV measurements were performed on a Jasco J-720 spectropolarimeter (Jasco LtD., Tokyo, Japan) in Jasco cylindrical cuvettes with a path length of 10 mm. 1 mg of chicken erythrocyte DNA (Reanal, Budapest, Hungary) was dissolved in 10 ml distilled water (stock solution, 0.1 mg/ml) and was further diluted to 0.033 mg/ml for the experiments. Tested substances were dissolved in DMSO (Sigma-Aldrich, Budapest, Hungary) in 5–10 mM concentration. All experiments were performed at ambient temperature.

2.3. Physicochemical calculations

For the prediction of some physicochemical parameters of our compounds, we have used the Calculator Plugins of ChemAxon. The Clog*P* values were calculated with all three methods and database of the software. The Clog*P* and solubility values are results in physiological pH = 7.4. See the corresponding homepage for detailed conditions of the calculations [33]. To explain the relationship between biodata and calculated physicochemical parameters the Lipinski approaches have been used [32].

2.4. Cell culture

MCF-7 human non-invasive breast adenocarcinoma cancer cells [26] were cultured in DMEM medium with 4.5 g/l glucose and 2 mM L-glutamine (Lonza, Verviers, Belgium). Jurkat human T lymphocyte leukemia cells [27] were cultured in RPMI 1640 medium with 2 mM L-glutamine (Lonza). All media were supplemented with 10% heat-inactivated FBS (Sigma, St. Louis, MO) and antibiotics 10 ml/l (penicillin-streptomycin 100 x, Sigma, St. Louis, MO).

2.5. Cytotoxicity test

Following the protocol of XTT cell viability assay (Biotium, Hayward, CA), the concentrations were 50.000 cells/ml (MCF-7) and 100.000 cells/ml (Jurkat) in the above described supplemented media. 100 μl of cell suspension was placed into each well of 96-well plates and incubated for 48 h in regular conditions (37 °C, 100% relative humidity and 5% CO_2). 5 μl solutions of curcumin and its analogs diluted in DMSO (Sigma, St. Louis, MO), added to each well to reach 10 nM, 100 nM, 1 μM, 10 μM and 20 μM final concentrations. After 24-h incubation in regular cell culture conditions, 25 μl activated XTT solution was mixed with media in the wells and consecutively incubated for 3 h. Finally, the absorbance was measured at a wavelength of 490 nm with DiaReader ELx800 (Dialab, Vienna, Austria) microplate reader. Results of curcumin and its analogs were compared to the DMSO controls with Student's t-test and statistical significance ($p < 0.05$) was calculated.

2.6. Experimental (logP)

RP-TLC log*P* determinations were performed by a slight modification of the previously optimized RP-TLC method used for determination of some chalcones and cyclic chalcone analogs [28,29]. Compounds of the calibration set (selected chalcones and cyclic chalcone derivatives, see the structures in "Supportive material") were synthesized and purified as described [37]. Their log*P* values were determined earlier [28,29]. Two compounds of the validation set (progesterone, diazepam) were of pharmacopoeial grade. All other reagents used were of analytical grade.

RP-TLC determination of the log*P* of the cyclic C_5-curcuminoid compounds **6**–**9** was performed on 20 cm × 20 cm plates precoated with 0.25 mm layers of silanized silica gel $60F_{254}$ (Merck, Germany; #5747). The plates were washed with methanol and dried before use. The samples of **6**–**9** were dissolved in 1:1 methanol-chloroform (c = 1 mg/cm^3) and 2 μl of these solutions were spotted on the plate. Methanol-water, 70 + 30 (v/v), was used as mobile phase. The paper-lined chromatographic chamber was saturated with the mobile phase for 30 min before use. After development (150 mm) the plates were dried and the chromatograms assessed visually under UV illumination (λ = 254 nm). Three TLC determinations were performed for each substance.

Some of the investigated molecules contain weakly basic functional groups. It was found, however, that they occur as non-ionized, neutral species under the experimental conditions.

2.7. Validation of the RP-TLC system

The optimized chromatographic system underwent validation prior to log*P* measurements. For this purpose, four molecules (progesterone, diazepam, chalcone and a chalcone derivative (Q-693)) with known log*P* values were tested. Comparison of their $logP_{TLC}$ values obtained in this work with previously published experimental log*P* data [28] resulted in rather good agreement. Thus, these four compounds were also added to the calibration set.

The $logP_{TLC}$ data obtained by our optimized and validated RP-TLC method are listed in Table 6. The log*P* data can provide a good basis for evaluation of structure-lipophilicity relationship for the examined compounds **6**–**9**. See "Supplementary data" for more details.

3. Results and discussion

3.1. Chemistry

The synthesis of our model compounds **6**–**9** for this SAR study was performed according to known methods involving the conditions of a Claisen-Schmidt condensation as depicted in Fig. 2. The nitrogen containing heterocyclic derivatives **7** and **8** have been prepared according to our new "one-pot" synthesis [22] starting from the corresponding β-ketoesters and aldehydes. Condensation reactions were carried out under basic or acidic conditions in good yields in a range of 75–90%. Formally, four different cyclic ketones, like 4-methylcyclohexanone (**1**), 4-piperidone (**2**), N-methyl-4-piperidone (**3**) or 4-hydroxycyclohexanone (**4**) and always the

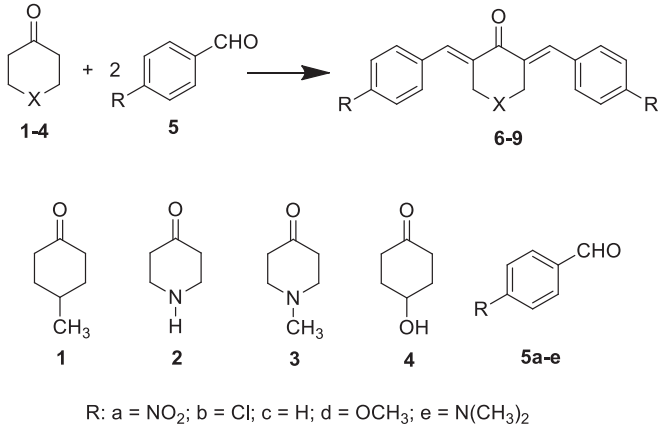

Fig. 2. Synthetic homo- and heterocyclic C_5-curcuminoid model compounds **6**–**9** with four different cyclanone cores and five aromatic substituents.

same five benzaldehydes (**5a-e**) have been transformed in these cross-aldol condensation reactions to form the desired model compounds **6**–**9**. Cyclanone **4** was prepared accordingly to our previously published method [23].

Our goal was on the one hand to prepare target compounds **6**–**9** with a small substituent in the central ring (X = CH-CH_3, N-H, N-CH_3 or CH-OH) due to the fact, that derivatives **7b** and **7c** (Fig. 3) turned out to be very promising antiproliferative agents. They have even been selected as standard lead compounds to be compared to newer promising agents [22 and references therein]. We selected five substituents onto the aromatic rings (nitro, chloro, hydrogen, methoxy, dimethylamino) on the other hand, in order to find the most optimal structure from the SAR analysis with the two substituents in the central and aromatic rings. In Fig. 3 we can see the structures of the twenty cyclic C_5-curcuminoid derivatives prepared for this study. Compounds **7b**, **7c**, **8b**, **8c** [22] and **9a-e** [23] were prepared by us previously together with the others (**6a-e**, **7a**, **7d**, **7e**, **8a**, **8d** and **8e**, see the experimental part) are in good accordance with the literature data in terms of their melting points and ^{1}H NMR spectra.

3.2. Cytotoxicity

The synthesized compounds were evaluated for their *in vitro* antiproliferative activity against MCF-7 human non-invasive breast adenocarcinoma cancer cells [26] and Jurkat human T lymphocyte leukemia cells [27] in an XTT cell viability assay. Inhibition of cell proliferation by these active compounds at various concentrations (10 nM, 100 nM, 1 μM, 10 μM and 20 μM) was measured, and their IC_{50} (the concentration that causes a 50% cell proliferation inhibition) values were calculated and are summarized in Table 1.

It was observed generally, that Jurkat leukemia cells were more susceptible to cytotoxic treatment in almost all cases compared to MCF-7 cells (Table 1). We have observed in eight cases, that the given compound was practically ineffective. Compounds **6e** and **8e** were ineffective on both cell lines. Although we did not use non-cancer cells for cytotoxicity tests, the difference in susceptibility of the two cell lines and of ineffective cases of these compounds is proof of their selective toxicity. We can state, however, that the majority of these compounds proved very good activity on cytotoxicity/viability tests. Many of them like **6a**, **7a**, **7b**, **7c**, **7e**, **8a**, **8b** and **9a** (**6a**, **7a**, **7c** and **8b** on both cell lines) were active even in the nanomolar range.

Moreover, many of them showed superior cytotoxic activity to Curcumin, namely compounds **7e**, **8b**, **7c**, **7a**, **7b** and **6a** on Jurkat cells while compounds **7a**, **8b**, **6a**, **8a** and **7c** on MCF-7 cell line. The previous sequence is important because it shows also the ranking of their IC_{50} values. The IC_{50} values of the most active compounds on Jurkat cells are between 0.14 (**7e**) and 0.40 (**6a**) μM while 0.12 (**7a**) and 0.81 (**7c**) μM on MCF-7 cells.

The relative potential, which shows the rate of dominance over curcumin of compounds in Table 1, is higher on MCF-7 cell lines in general. For example, **7e** on Jurkat and **7a** on MCF-7 cells have a similar IC_{50} value (0.14 and 0.12 respectively), but the relative potential is different. It is 6.79 for **7e** on Jurkat and 81.33 for **7a** on MCF-7. This means, that **7a** is the most potent congener compared to curcumin. It is important to emphasize, that derivatives **6a**, **7a**, **7c** and **8b** possess cytotoxicity on both cell lines. We can draw a very positive conclusion that our model compounds are showing selective toxicity with different relative potentials.

The β-dienone moiety, which serves as the primary pharmacophore function (Fig. 4, **A**) in the structure of our compounds **6**–**9** is the same in all derivatives. In order to compare changes in activity after structural modifications on the central ring and on the aromatic benzylidene rings we have created a “heat-map” including the structures of the compounds with substituents on the central and aromatic rings, IC_{50} values of our cyclic C_5-curcuminoids and

Table 1
In vitro antiproliferative activities of model-compounds against Jurkat and MCF-7 cancer cell lines in terms of their IC_{50} (the concentration that causes a 50% cell proliferation inhibition) values in micromoles and relative potentials related to Curcumin.

Compound	Jurkat		MCF-7	
	IC_{50}[μM]	Relative pot.[a]	IC_{50}[μM]	Relative pot.[a]
Curcumin	0.95	1.00	9.76	1.00
6a	0.40	2.38	0.49	19.92
6b	6,59	0.14	17.00	0.57
6c	4.00	0.24	9.80	0.996
6d	2.89	0.33	8.77	1.32
6e	>20	not relevant	>20	not relevant
7a	0.32	2.97	0.12	81.33
7b	0.36	2.64	>20	not relevant
7c	0.24	3.96	0.81	12.34
7d	10.32	0.09	5.87	1.66
7e	0.14	6.79	9.80	0.996
8a	1.00	0.95	0.75	13.32
8b	0.21	4.52	0.43	22.70
8c	1.49	0.64	2.38	4.31
8d	9.32	0.10	>20	not relevant
8e	>20	not relevant	>20	not relevant
9a	0.88	1.37	1.64	5.95
9b	1.99	0.48	>20	not relevant
9c	2.30	0.41	8.71	1.32
9d	10.50	0.09	11.31	0.86
9e	19.85	0.05	>20	not relevant

[a] Relative potential: IC_{50} value of curcumin divided by the IC_{50} value of the compound.

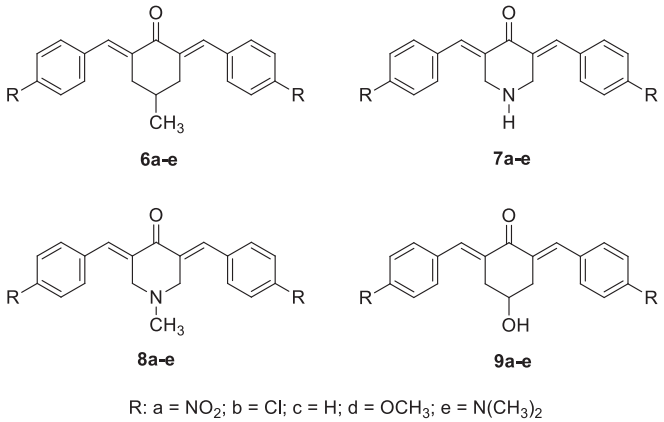

Fig. 3. Structures of the twenty homo- and heterocyclic C_5-curcuminoids prepared for this SAR study.

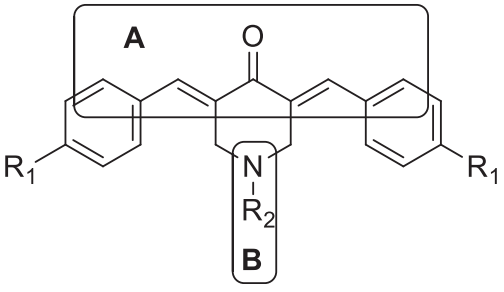

Fig. 4. The primary (**A**) and secondary (**B**) pharmacophore functions of cyclic C_5-curcuminoids.

the two cell lines (Table 2). The smaller IC_{50} values (higher antiproliferative activity) are in red whilst the bigger IC_{50} values (lower activity) are in blue. The others in between are in yellow and green.

Our first conclusion is that the heterocyclic derivatives **7** and **8** exhibited more pronounced antiproliferative activities compared to their homocyclic counterparts **6** and **9**. This fact promotes our earlier findings [22,23] on such heterocyclic C_5-curcuminoids including compounds **7b**, **7c**, **8b** and **8c** [22] or **9a-e** [23]. The reference standard was cisplatin in both of these two studies. The position opposite to the ketone carbonyl on the central cyclanone ring, being an auxiliary binding ability (secondary pharmacophore, Fig. 4, **B**) to the *in vivo* biological site of action, has a great influence on the cytotoxicity of these compounds. In other words, the binding strength of these cyclic C_5-curcuminoids to the biological site of action is stronger when there is a suitable substituent and/or a nitrogen heteroatom at this position. This moiety on the central cyclanone ring (Fig. 4, **B**) is able to enhance the interaction between the cyclic C_5-curcuminoids and their biological place of action in the cancer cell. This is visible on the example of **6b** and **8b**: the cytotoxic activity increases on both cell lines (see the corresponding IC_{50} values) after the nitrogen atom "appears" in the homocycle of **6b** to form the heterocyclic **8b** counterpart (Table 2). A similar example is the exchange of the NH functional group of compound **7c** to an OH in **9c**.

The second conclusion is that the electron withdrawing *p*-chloro and especially *p*-nitro substituents on the benzylidene parts are dominating the *p*-methoxy or *p*-dimethylamino electron donor substituents. For example, compound **6a** with a nitro group showed 0.40 μM IC_{50} value on Jurkat cells, whilst **6e** with a dimethylamino substituent was practically ineffective. The same is true on the MCF-7 cell line about **6a** and **6e**. Apart from some exceptions, similar examples are there in Table 2. A definite structure/activity relation was discovered comparing the average IC_{50} values of the five substituents (nitro, chloro, hydrogen, methoxy and dimethylamino) on benzylidene moieties (Table 2). The best performer is the nitro-substituted benzylidene group (**6a**, **7a**, **8a** and **9a**) with IC_{50} values ranging from 0.12 to 1.64 μM. The second in this sequence is the unsubstituted benzylidene group (**6c**, **7c**, **8c** and **9c**), the third is the chloro-substituted **6b**, **7b**, **8b** and **9b**. The last two positions remain to the methoxy (**d**) and dimethylamino (**e**) substituents with average IC_{50} values of 8.43 and 9.93 μM respectively.

Experimental and calculated data in Tables 1 and 2, in relation to the two moieties **A** and **B** (Fig. 4) suggest that there is an electron withdrawing substituent on the benzylidene groups and a nitrogen heteroatom in the optimal structure for the optimal antiproliferative activity. From this SAR analysis, it is noteworthy that we could not find (apart from a few exceptions like **6a**, **7a** or **6e**, **8e**) a very strong relationship between the IC_{50} values of the two cell lines. The two cell lines correlate neither the Pearson correlation nor the Kendall coefficient of concordance. Our results on the corresponding calculations showed a Kendall coefficient match bigger than 1. It was 1.75, which may mean interestingly two different ways of biological action on the two different cancer cell lines.

3.3. Physicochemical investigations

3.3.1. Experimental logP (logP)

On the basis of our former results [28,29], we designed and performed experiments in order to obtain experimental log*P* values of cyclic C_5-curcuminoid compounds **6**–**9**. The method we developed, validated and applied is a chromatographic measurement in a reversed phase thin-layer chromatographic (RP-TLC) setting. The theoretical base for the determination of log*P* by chromatographic methods is the relation between the partition coefficient (measured with a shake-flask) and a chromatographic retention parameter (R_M for RP-TLC) based on liquid/liquid partition. R_M values (calculated using R_f) are in a linear correlation with log*P* values in a suitable chromatographic system according to the

$$\log P = aR_M + b$$

equation. The essence of chromatographic log*P* determination is thus the determination of the regression parameters of the above equation by using a set of standards (calibration set) with known octanol/water log*P* values. Based on this equation the experimental log*P* of other compounds can be calculated. See experimental for details.

Results from the RP-TLC measurements for experimental log*P* data are summarized in Table 3. These data revealed a clear, consistent structure dependency of the measured log*P* values. The model molecules are highly lipophilic, as might be expected from their chemical structures. They contain an extended lipophilic carbon skeleton with aromatic moieties, which are compensated only a little bit by the polarity of the carbonyl group. Polarity of the structures is under slight influence also by the aromatic substituents.

Apart from some exceptions like **7e** or **9a**, lipophilicity is decreasing in the sequence of **6**, **7**, **8** and **9**. This tendency is visible in general (see the average values) and in parts (see the rows in Table 3). On the other hand, lipophilicity is growing from nitro toward dimethylamino substituent (see the columns in Table 3) in the sequence of **a**, **c**, **d**, **b** and **e** along with exceptions like **7d** or **9a**. The exceptions mentioned before are due to a possible self-dimerization with H-bonds of compounds **7** or **9** respectively,

Table 2
The IC_{50} "heat-map" of compounds **6**–**9**. Curcumin IC_{50}: Jurkat – 0.95; MCF-7 – 9.76 μM.

Compound	R=	nitro	chloro	H	methoxy	dimethylamino
	Cell line:	a	b	c	d	e
6	Jurkat	0.40	6.59	4.00	2.89	>20
($CH\text{-}CH_3$)	MCF-7	0.49	17.00	9.80	8.77	>20
7	Jurkat	0.32	0.36	0.24	10.32	0.14
(N-H)	MCF-7	0.12	>20	0.81	5.87	9.80
8	Jurkat	1.00	0.21	1.49	9.32	>20
($N\text{-}CH_3$)	MCF-7	0.75	0.43	2.38	>20	>20
9	Jurkat	0.88	1.99	2.30	10.50	19.85
(CH-OH)	MCF-7	1.64	>20	8.71	11.31	>20
	Average:	0.70	4.43	3.72	8.43	9.93

Table 3
Experimental log*P* values (±sample standard deviation), determined by RP-TLC method.

Compounds: R =	6:	7:	8:	9:
a: $-NO_2$	4.70 ± 0.01	3.22 ± 0.30	3.31 ± 0.03	3.62 ± 0.02
c: −H	5.82 ± 0.06	4.11 ± 0.17	4.14 ± 0.04	3.36 ± 0.01
d: $-OCH_3$	5.98 ± 0.07	5.10 ± 0.32	4.57 ± 0.06	3.57 ± 0.04
b: −Cl	6.40 ± 0.05	4.75 ± 0.12	5.01 ± 0.09	4.28 ± 0.01
e: $-N(CH_3)_2$	6.75 ± 0.07	7.29 ± 0.02	5.69 ± 0.15	4.04 ± 0.13
Average:	5.93	4.89	4.54	3.77

through their polar functional groups (NH or OH) [30,31]. This possible dimerization makes them less polar and so more lipophilic under the conditions of the measurement. The most lipophilic substance is **7e** with an extreme high log*P* value.

Our goal was also to determine if there was a correlation between the obtained log*P* data and the pharmacological activity of model compounds **6**–**9**. Therefore, we collected the experimental log*P* and the corresponding IC_{50} values into Table 4. In order to have a more detailed insight, the data from Table 4 underwent calculations according to Pearson correlation and Kendall coefficient of concordance. As a result of our calculations, we may conclude, that there was no consistent linear or logarithmic relation that could be established between antiproliferative activity and lipophilicity of our model compounds in this study. This fact does not mean, however, that there is no positive correlation between the nature of the structure and the biological activity at all.

We can state for example that compounds with IC_{50} value under the median value of 2.15 μM Jurkat or 9.29 μM MCF-7 (which means good antiproliferative action) together with lower log*P* value of the median 4.63 are promising molecules. Compounds like this in Table 4 are **7a**, **7c**, **8a**, **8c** and **9a** under Jurkat line or **7a**, **7c**, **8a**, **8c**, **9a** and **9c** under the MCF-7 line. The log*P* of these most effective compounds are in the range of 3.22 and 4.63. There are derivatives with higher log*P* value, which are practically ineffective compounds like **6e** or **8e**. There is only one compound (**7e**) in conflict with this (Table 4). The majority of these compounds are in good accordance with Lipinski's rule [32].

To visualize the relationship between experimental log*P* and IC_{50} data we have plotted them against each other. The diagrams on the two cancer cell lines are in Fig. 5. The most promising compounds are in blue. They have lower lipophilicity with higher antiproliferative activity (smaller IC_{50} values). Derivatives represented with red spots are more lipophilic with lower activity, except **6c**, **6d** and **7e** on Jurkat cells. The most promising compound is **7a**, which is the most potent on both cell lines with the lowest lipophilicity, which is also important from a pharmacokinetic point of view.

Table 4
Collected experimental data from log*P* and IC_{50} measurements.

Compound	log*P*	IC_{50} [μM]	
		Jurkat	MCF-7
6a	4.70	0.40	0.49
6b	6.40	6.59	17.00
6c	5.82	4.00	9.80
6d	5.98	2.89	8.77
6e	6.75	>20	>20
7a	3.22	0.32	0.12
7b	4.75	0.36	>20
7c	4.11	0.24	0.81
7d	5.10	10.32	5.87
7e	7.29	0.14	9.80
8a	3.31	1.00	0.75
8b	5.01	0.21	0.43
8c	4.14	1.49	2.38
8d	4.57	9.32	>20
8e	5.69	>20	>20
9a	3.62	0.88	1.64
9b	4.28	1.99	>20
9c	3.36	2.30	8.71
9d	3.57	10.50	11.31
9e	4.04	19.85	>20
Median:	4.63	2.15	9.29

3.3.2. *Predictive physicochemical calculations (ClogP, solubility in water and 3D shape)*

For an evaluation of some physicochemical properties (compared to curcumin), the parameters of the synthesized compounds were computed. Just as in our previous studies [22,23] ChemAxon's Marvin Suite Plugins were used for all of the calculations [33]. Calculated log*P* was determined according to three different methods of Marvin's calculator plus the average value (Table 5).

Number of hydrogen bond forming ability of the structures,

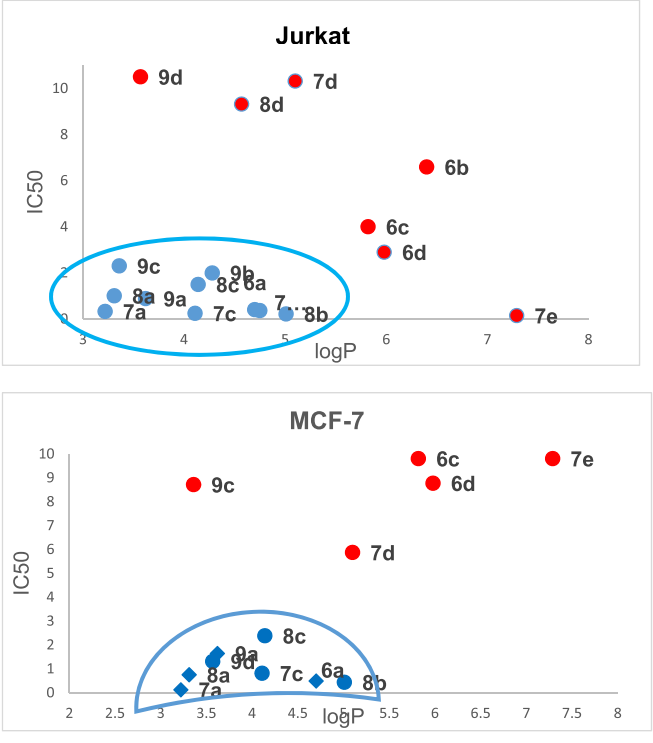

Fig. 5. Relationship between antiproliferative activity and lipophilicity of compounds **6**–**9**. Experimental log*P* and IC_{50} data of the effective derivatives are plotted against each other.

Table 5
Computed physicochemical parameters of the investigated compounds were undertaken. Calculated partition coefficient (Clog*P*) values were determined according to three methods (VG, KLOP, PHYS) of Marvin Suite [33]. Predicted solubility at pH = 7.4 of the compounds is considered to be "Low" in this table, when it does not exceed 0.01 and is moderate if it was 0.01–0.06 mg/ml in water.

Compound	MW	VG	ClogP	PHYS	Average	log*P*	H-bond	Solubility	IC_{50}	
			KLOP			(TLC)			Jurkat	MCF-7
6a	378.38	6.20	5.58	5.51	5.76	4.70	5	Low	0.40	0.49
6b	357.27	7.33	7.04	6.91	7.09	6.40	1	Low	6.59	17.00
6c	288.39	6.30	5.76	5.59	5.88	5.82	1	Low	4.00	9.80
6d	348.44	5.79	5.49	5.43	5.57	5.98	3	Low	2.89	8.77
6e	374.53	6.82	5.73	5.75	6.10	6.75	3	Low	>20	>20
7a	365.35	4.30	3.65	3.39	3.78	3.22	7	Low	0.32	0.12
7b	344.24	5.43	5.11	4.78	5.11	4.75	3	Low	0.36	>20
7c	275.35	4.39	3.83	3.47	3.90	4.11	3	Low	0.24	0.81
7d	335.40	3.89	3.56	3.30	3.58	5.10	5	Moderate	10.32	5.87
7e	361.49	4.92	3.80	3.63	4.12	7.29	5	Moderate	0.14	9.80
8a	379.37	4.66	3.93	3.89	4.16	3.31	6	Low	1.00	0.75
8b	358.26	5.79	5.40	5.28	5.49	5.01	2	Low	0.21	0.43
8c	289.38	4.76	4.12	3.97	4.28	4.14	2	Low	1.49	2.38
8d	349.43	4.25	3.85	3.80	3.97	4.57	4	Low	9.32	>20
8e	375.52	5.28	4.08	4.13	4.50	5.69	4	Moderate	>20	>20
9a	380.36	4.51	3.82	3.94	4.09	3.62	7	Low	0.88	1.64
9b	359.25	5.64	5.28	5.33	5.42	4.28	3	Low	1.99	>20
9c	290.36	4.61	4.01	4.02	4.21	3.36	3	Low	2.30	8.71
9d	350.41	4.10	3.73	3.85	3.90	3.57	5	Low	10.50	11.31
9e	376.50	5.14	3.97	4.17	4.43	4.04	5	Moderate	19.85	>20
Curcumin	368.13	3.95	3.65	3.68	3.76	4.12	9	Moderate	0.95	9.76

Table 6
LogP_{SF} and logP_{TLC} values of the compounds of the validation set.

	logP_{SF}	logP_{TLC}	Δlog*P*
Chalcone	3.62	3.62	0
Q693	3.74	3.77	0.03
Progesterone	3.54	3.67	0.13
Diazepam	2.82	3.05	0.23

including donor or acceptor, and solubility in water (mg/ml) were also calculated. We couldn't find any rationale among the predicted physicochemical data in Table 5 to explain the difference between the antiproliferative activity of curcumin and our model compounds **6**–**9**. There are only some slight variations in the values of the data listed in Table 5. This can not be the cause of the great difference in pharmacological activity between curcumin and our cyclic C5-curcuminoids. The reason for this must be somewhere else, which leads us to investigate further in this direction.

Data in Table 5 together with our earlier findings [22,23] however show that the software [33] we used in our research is useful and beneficial.

Computed structures were also cleaned into 3D shape by the software used [33]. Compounds **8c** and **9c** as examples are available in their "ball and stick" model without their hydrogen atoms in Fig. 6. What we can see in general is that the two benzene rings in a molecule are not in the same plane. It is also visible, that the central ring (4-piperidone or 4-hydroxycyclohexanone respectively) is located in a third plane. These three planes occupy a "close-to-planar" molecular shape. It is important to note that the central rings are almost planar. Only the atom opposite to the carbonyl function is out of the plane in an envelope-like form. Finally, the cyclic β-dienone moiety in this cross-conjugated system keeps the conformation of these molecules fixed.

3.4. DNA binding

CD is a reliable tool for the detection of DNA binding of ligands, like drugs or any other different molecules. The appearance of the induced circular dichroism signal (ICD) is definitive proof of the interaction. In addition, shifts in the DNA bands are also indicative of the binding [34,35].

There is little known about the DNA binding of cyclic C_5-curcuminoids. However, we know more about curcumin in this respect. It is known from *in vitro* experiments for example, that curcumin appears in the nucleus of cultured glioma cells after incubation. It was revealed that nuclear homing is not a result of curcumin's DNA binding [36]. The temporal relationship of curcumin's apoptotic induction effect and its nuclear homing is under investigation to acquire details about the mechanism of action. This fact among others prompted us to initiate measurements to see possible interactions between C_5-curcuminoids and DNA. For this reason, we conducted circular dichroism spectroscopic

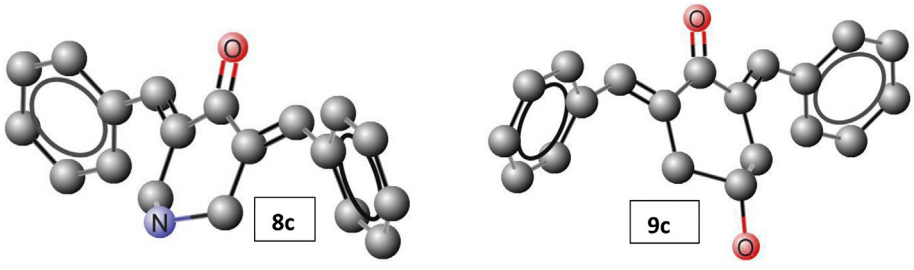

Fig. 6. "Ball and stick" 3D models of compounds **8c** and **9c** without hydrogen atoms.

investigations on the synthesized cyclic C_5-curcuminoid derivatives in series **6**–**9** using natural DNA.

Curcumin, as well as 20 cyclic C_5-curcuminoid derivatives **6**–**9** were tested on chicken erythrocyte DNS. In the CD spectrum of curcumin, a large ICD band appeared in the ligand's absorption region, showing a strong interaction between the ligand molecule and the chicken erythrocyte polynucleotide (Fig. 7). It also caused some minor shift in the DNA band, meaning the double helical structure is slightly distorted (Fig. 7). Those derivatives containing either aliphatic or aromatic nitrogen showed signs of interaction - a weak ICD sign appeared in the recorded spectra for example in the case of dimethylamino substituted **6e**, **7e**, **8e** and **9e** (Fig. 7). DNA bands did not change significantly at the same time, indicating that the polynucleotide remains in its native B-form. The binding is most probably the result of the weak ionic interaction of the nitrogen atoms from the cyclic C_5-curcuminoid structure with the phosphate groups of DNA. In the case of other derivatives with no nitrogen atom in their structure neither an ICD signal, nor a shift in the DNA bands was detected, indicating that no interaction occurs between the molecules and DNA (Fig. 7).

Although it would be consistent with an ability of these curcuminoids **6**–**9** to adopt a "close-to-planar" molecular shape (Fig. 6), in contrast to curcumin, none of them showed stronger interaction with the DNA used in this study. It would be conceivable that the very active inhibitors in Table 2 show diverse interaction compared to the practically ineffective counterparts (Table 1). However, compounds in these series showed similar properties under CD conditions that make it possible to generalize: based on these data we conclude that these derivatives do not bind to DNA *in vitro*. Due to this finding, we can disclose that the antiproliferative activity of these cyclic C_5-curcuminoids is not due to their interaction with DNA.

The CD spectra of compounds **6**–**9** can be found in the "Supplementary data" section.

4. Conclusions

The chemical susceptibility of the β-diketone linker between the

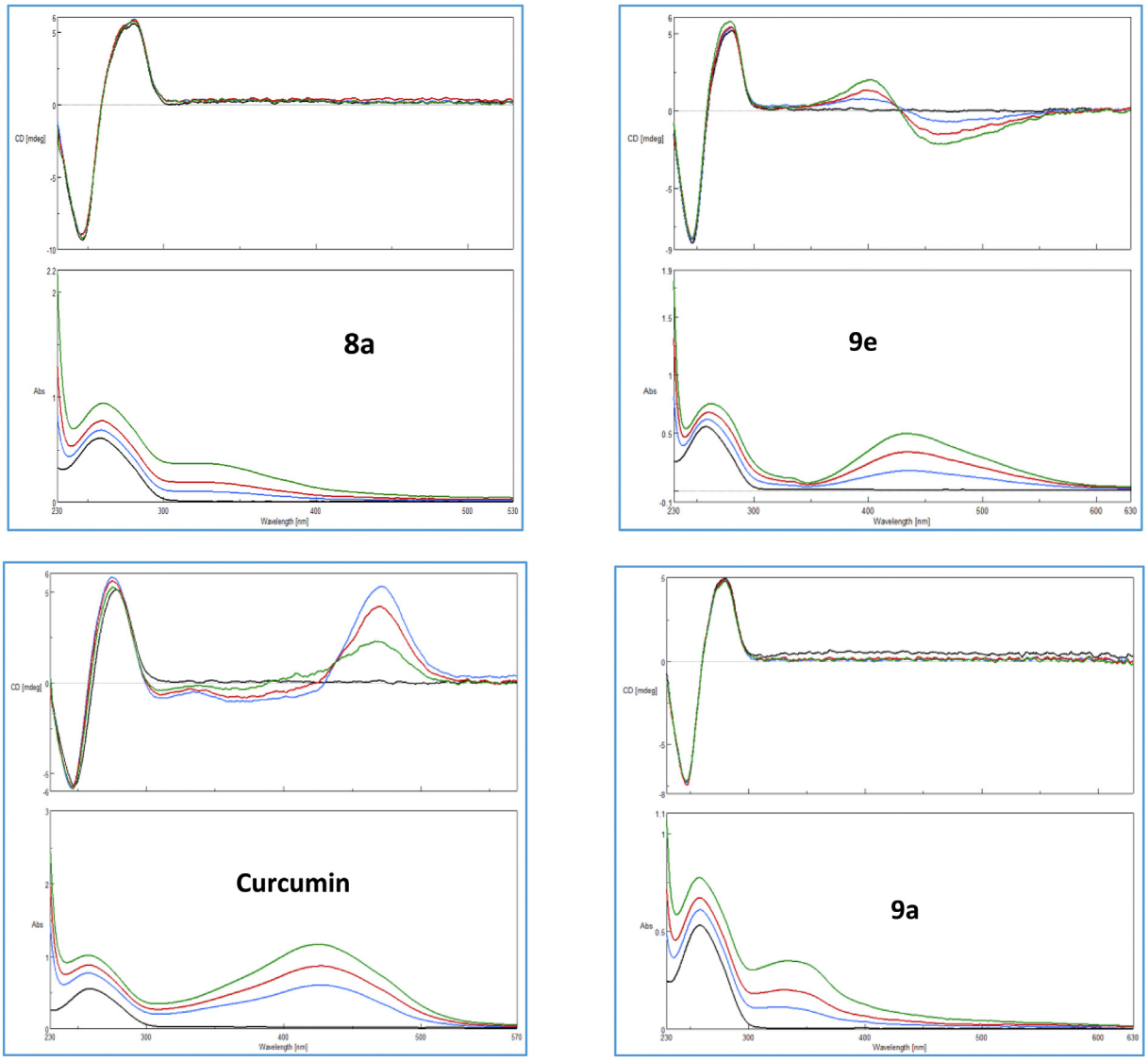

Fig. 7. Selected CD and UV titration of 0.033 mg/ml chicken erythrocyte DNA (black, lowest curve) with 5 mM curcumin or cyclic C_5-curcuminoid stock solution (final concentrations are 16.66 μg/ml, 25 μg/ml and 33.33 μg/ml respectively). Strong interaction of curcumin, very weak interaction of **9e**. The other derivatives remain intact, like for example **8a** or **9a**.

two aromatic rings in the structure of curcumin to hydrolysis and metabolism [24,25] has made it a crucial point to investigate structurally modified analogs of curcumin without such shortcomings. These well-known shortcomings at the same time are the possible reasons for the drawbacks in the bioavailability of curcumin [3]. On this basis and as a continuation of our former SAR studies [22,23] we have designed and synthesized twenty cyclic C_5-curcuminoids (**6**–**9**), the truncated forms of curcumin in order to have a deeper insight into the impact of structural modifications over cytotoxic activity and/or physicochemical parameters of our model compounds **6**–**9**. The β-dienone linker of these C_5-curcuminoids is stable and has the same role as the β-diketone moiety of curcumin such as the primary pharmacophore function. We have modified the polarity/lipophilicity of this β-dienone linker by introducing five different substituents (nitro, chloro, hydrogen, methoxy and dimethylamino, respectively) onto the aromatic rings dividing the group (**6**–**9**) into five subgroups (**a**, **b**, **c**, **d** and **e**). The four different cyclanons (**1**–**4** in Fig. 2) divided the group of these model compounds further into four additional subgroups (**6**–**9**). The four subgroups have selected moieties in the central cyclanone ring in the position opposite the carbonyl function, and these moieties are filling the role of the secondary pharmacophore of these compounds (Fig. 4). As a conclusion, we can state that the structural modifications in the primary and secondary pharmacophore of these model molecules resulted in clear correlations in our SAR analysis. Experimental and calculated data in Tables 1 and 2, in relation to the two moieties **A** and **B** (Fig. 4) suggest that there is an electron withdrawing substituent on the benzylidene groups and a nitrogen heteroatom in the optimal structure for the optimal antiproliferative activity. The IC_{50} values of the antiproliferative activity dropped to the minimum compared to curcumin, even to submicromolar in cases close to the optimal structure. The physicochemical parameters such as molecular weight, polarity, log*P* and solubility of these compounds are in good accordance with Lipinski's rule [32]. The most promising compound is **7a**, which is the most effective (IC_{50} = 0.12–0.32 μM), most potent (80 times of curcumin) with the lowest lipophilicity (experimental log*P* = 3.22) which is important also from a pharmacokinetic point of view. There was no sign (or very weak if at all) of interaction between cyclic C_5-curcuminoids **6**–**9** and DNA in the CD spectra. Therefore, we can also conclude that there is no risk for such possible and serious side effects from this source in the case of these curcuminoids. This fact is an advantage over curcumin if we compare the results of our circular dichroism (CD) investigations. These findings increase the knowledge about such cyclic C_5-curcuminoids in order to find the optimal structure in terms of antiproliferative activity and potential.

Declaration of competing interest

The authors declare no conflict of interest.

Acknowledgments

HI acknowledges support from the University of Pécs, Faculty of Medicine Research Fund PTE ÁOK-KA-34039-12/10–11.

Appendix A. Supplementary data

Supplementary data to this article can be found online at https://doi.org/10.1016/j.molstruc.2019.127661.

References

[1] F.E. Koehn, G.T. Carter, The evolving role of natural products in drug discovery, Nat. Rev. Drug Discov. 4 (2005) 206–220.
[2] S.C. Gupta, S. Patchva, B.B. Aggarwal, Therapeutic roles of curcumin: lessons learned from clinical trials, AAPS J. 15 (1) (2013) 195–218.
[3] A.S. Oliveira, E. Sousa, M.H. Vasconcelos, M. Pinto, Curcumin: a natural lead for potential new drug candidates, Curr. Med. Chem. 22 (2015) 4196–4232.
[4] B.B. Aggarwal, A. Kumar, A.C. Bharti, Anticancer potential of curcumin: preclinical and clinical studies, Anticancer Res. 23 (2003) 363–398.
[5] T. Masuda, A. Jitoe, J. Isobe, N. Nakatani, S. Yonemori, Anti-oxidative and anti-inflammatory curcumin-related phenolics from rhizomes of *Curcuma domestica*, Phytochemistry 32 (1993) 1557–1560.
[6] J.L. Jiang, X.L. Jin, H. Zhang, X. Su, B. Qiao, Y.J. Yuan, Identification of antitumor constituents in curcuminoids from *Curcuma longa* L. based on the composition-activity relationship, J. Pharm. Biomed. Anal. 70 (2012) 664–670.
[7] A. Kohyama, H. Yamakoshi, S. Hongo, N. Kanoh, H. Shibata, Y. Iwabuchi, Structure-activity relationships of the antitumor C_5-curcuminoid GO-Y030, Molecules 20 (2015) 15374–15391.
[8] A. Kohyama, M. Fukuda, S. Sugiyama, H. Yamakoshi, N. Kanoh, C. Ishioka, H. Shibatac, Y. Iwabuchi, Reversibility of the *thia*-Michael reaction of cytotoxic C_5-curcuminoid and structure–activity relationship of bis-thiol-adducts thereof, Org. Biomol. Chem. 14 (2016) 10683–10687.
[9] S. Mapoung, S. Suzuki, S. Fuji, A. Naiki-Ito, H. Kato, S. Yodkeeree, C. Ovatlarnporn, S. Takahashi, P. Limtrakul, Cyclohexanone curcumin analogs inhibit the progression of castration-resistant prostate cancer *in vitro* and *in vivo*, Cancer Sci. 110 (2019) 596–607.
[10] K. Selvendiran, S. Ahmed, A. Dayton, M.L. Kuppusamy, M. Tazi, A. Bratasz, L. Tong, B.K. Rivera, T. Kálai, K. Hideg, P. Kuppusamy, Safe and targeted anticancer efficacy of a novel class of antioxidant-conjugated difluoro-diarylidenylpiperidones. Differential cytotoxicity in healthy and cancer cells, Free Radic. Biol. Med. 48 (2010) 1228–1235.
[11] A. Dayton, K. Selvendiran, M.L. Kuppusamy, B.K. Rivera, S. Meduru, T. Kálai, K. Hideg, P. Kuppusamy, Cellular uptake, retention and bio-adsorption of HO-3867, a fluorinated curcumin analog with potential antitumor properties, Cancer Biol. Ther. 10 (2010) 1027–1032.
[12] T. Kálai, M.L. Kuppusamy, M. Balog, K. Selvendiran, B.K. Rivera, P. Kuppusamy, K. Hideg, Synthesis of N-substituted 3,5-bis(arylidene)-4-piperidones with high antitumor and antioxidant activity, J. Med. Chem. 54 (2011) 5414–5421.
[13] N. Li, W. Xin, B. Yao, C. Wang, W. Cong, F. Zhao, H. Li, Y. Hou, Q. Meng, G. Hou, Novel dissymmetric 3,5-bis(arylidene)-4-piperidones as potential antitumor agents with biological evaluation *in vitro* and *in vivo*, Eur. J. Med. Chem. 147 (2018) 21–33.
[14] Q. Chen, Y. Hou, G. Hou, J. Sun, N. Li, W. Cong, F. Zhao, H. Li, C. Wang, Design, synthesis, anticancer activity and cytotoxicity of novel 4-piperidone/cyclohexanone derivatives, Res. Chem. Intermed. 42 (2016) 8119–8130.
[15] S. Das, U. Das, A. Varela-Ramirez, C. Lema, R.J. Aguilera, J. Balzarini, E. De Clerck, S.G. Dimmock, D.K.J. Gorecki, J.R. Dimmock, Bis[3,5-bis(benzylidene)-4-oxo-1-piperidinyl]amides: a novel class of potent cytotoxins, ChemMedChem 6 (2011) 1892–1899.
[16] S. Das, U. Das, H. Sakagami, N. Umemura, S. Iwamoto, T. Matsuta, M. Kawase, J. Molnár, J. Serly, D.K.J. Gorecki, J.R. Dimmock, Dimeric 3,5-bis(benzylidene)-4-piperidones: a novel cluster of tumour-selective cytotoxins possessing multidrug-resistant properties, Eur. J. Med. Chem. 51 (2012) 193–199.
[17] M. Hossain, U. Das, N. Umemura, H. Sakagami, J. Balzarini, E. De Clercq, M. Kawase, J.R. Dimmock, Tumour-specific cytotoxicity and structure-activity relationships of novel 1-[3-(2-methoxyethylthio)propionyl]-3,5-bis(benzylidene)-4-piperidones, Bioorg. Med. Chem. 24 (10) (2016) 2206–2214.
[18] X. Yuan, H. Li, H. Bai, Z. Su, Q. Xiang, C. Wang, B. Zhao, Y. Zhang, Q. Zhang, Y. Chu, Y. Huang, Synthesis of novel curcumin analogues for inhibition of 11b-hydroxysteroid dehydrogenase type 1 with anti-diabetic properties, Eur. J. Med. Chem. 77 (2014) 223–230.
[19] U. Das, R.K. Sharma, J.R. Dimmock, 1,5-Diaryl-3-oxo-1,4-pentadienes: a case for antineoplastics with multiple targets, Curr. Med. Chem. 16 (2009) 2001–2020.
[20] M.V. Koonammackal, U.V.N. Nellipparambil, C. Sudarsanakumar, Molecular dynamics simulations and binding free energy analysis of DNA minor groove complexes of curcumin, J. Mol. Model. 17 (2011) 2805–2816.
[21] C.N. N'soukpoé-Kossi, P. Bourassa, J.S. Mandeville, L. Bekale, H.A. Tajmir-Riahi, Structural modeling for DNA binding to antioxidants resveratrol, genistein and curcumin, J. Photochem. Photobiol. B Biol. 151 (2015) 69–75.
[22] I. Huber, I. Zupkó, I.J. Kovács, R. Minorics, G. Gulyás-Fekete, G. Maász, P. Perjési, Synthesis and antiproliferative activity of cyclic arylidene ketones: a direct comparison of monobenzylidene and dibenzylidene derivatives, Monatsch. Chem. 146 (2015) 973–981.
[23] I. Huber, I. Zupkó, A. Gyovai, P. Horváth, E. Kiss, G. Gulyás-Fekete, J. Schmidt, P. Perjési, A novel cluster of C_5-curcuminoids: design, synthesis, *in vitro* antiproliferative activity and DNA binding of bis(arylidene)-4-cyclanone derivatives based on 4-hydroxycyclohexanone scaffold, Res. Chem. Intermed. 45 (2019) 4711–4735.
[24] Y. Zhang, Z. Liu, J. Wu, B. Bai, H. Chen, Z. Xiao, L. Chen, Y. Zhao, H. Lum, Y. Wang, H. Zhang, G. Liang, New MD2 inhibitors derived from curcumin with improved anti-inflammatory activity, Eur. J. Med. Chem. 148 (2018) 291–305.
[25] G.Y. Liu, C.C. Jia, P.R. Han, J. Yang, 3,5-Bis(2-fluorobenzylidene)-4-piperidone induce reactive oxygen species-mediated apoptosis in A549 cells, Med. Chem. Res. 27 (2018) 128–136.
[26] K.A. Graham, C.L. Richardson, M.D. Minden, J.M. Trent, R.N. Buick, Varying

degrees of amplification of the N-ras oncogene in the human breast cancer cell line MCF-7, Cancer Res. 45 (5) (1985) 2201–2205.
[27] Zs Rozmer, T. Berki, G. Maász, P. Perjési, Different effects of two cyclic chalcone analogues on redox status of Jurkat T cells, Toxicol. In Vitro 28 (8) (2014) 1359–1365.
[28] K. Takács-Novák, P. Perjési, J. Vámos, Determination of logP for biologically active chalcones and cyclic chalcone analogs by RPTLC, JPC-J. Planar Chrom. 14 (2001) 42–46.
[29] Zs Rozmer, P. Perjési, K. Takács-Novák, Application of RP-TLC for logP determination of isomeric chalcones and cyclic chalcone analogues, J. Planar Chromatogr. Mod. TLC 19 (2006) 124–128.
[30] A. Fonari, E.S. Leonova, M.V. Makarov, I.S. Bushmarinov, I.L. Odinets, M.S. Fonari, M.Y. Antipin, T.V. Timofeeva, Experimental and theoretical structural study of (3E,5E)-3,5-bis-(benzylidene)-4-oxopiperidinium mono- and (3E,5E)-3,5-bis-(4-N,N-dialkylammonio)benzylidene)-4-oxopiperidinium trications, J. Mol. Struct. 1001 (2011) 68–77.
[31] P. Lagisetti, D.R. Powell, V. Avasthi, Synthesis and structural determination of 3,5-bis(2-fluorobenzylidene)-4-piperidone analogs of curcumin, J. Mol. Struct. 936 (2009) 23–28.
[32] C.A. Lipinski, F. Lombardo, B.W. Dominy, P.J. Feeney, Experimental and computational approaches to estimate solubility and permeability in drug discovery and development settings, Adv. Drug Deliv. Rev. 46 (2001) 3–26.
[33] Calculator Plugins were used for structure property prediction and calculation, Marvin Suite 15.2.23, ChemAxon, http://www.chemaxon.com.
[34] S. Allenmark, Induced circular dichroism by chiral molecular interaction, Chirality 15 (5) (2003) 409–422.
[35] E. Kiss, A. Mirzahosseini, A. Hubert, A. Ambrus, L. Őrfi, P. Horváth, DNA binding of sunitinib: spectroscopic evidence via circular dichroism and nuclear magnetic resonance, J. Pharm. Biomed. Anal. 150 (2018) 355–361.
[36] M. Ghosh, R.O. Ryan, Curcumin homing to the nucleolus: mechanism for initiation of an apoptotic program, J. Nutr. Biochem. 25 (2014) 1117–1123.
[37] J.R. Dimmock, N.M. Kandepu, A.J. Nazarali, T.P. Kowalchuk, N. Motaganahalli, J.W. Quail, P.A. Mykytiuk, G.F. Audette, L. Prasad, P. Perjési, T.M. Allen, C.L. Santos, J. Szydlowski, E. De Clercq, J. Balzarini, Conformational and quantitative Structure–Activity relationship study of cytotoxic 2-arylidenebenzocycloalkanones, J. Med. Chem. 42 (1999) 1358–1367.
[38] S. Shruti, O.P. Chourasia, Synthesis, characterization and evaluation of antitubercular and antimicrobial activities of new thiazole derivatives, Intern. J. Pharm. Res. Bio-Science 4 (1) (2015) 265–276.
[39] G.H. Mahdavinia, M. Mirzazadeh, Fast, facile and convenient synthesis of α,α-bis(substituted-arylidene) cycloalkanones, an improved protocol, J. Chem. 9 (1) (2012) 49–54.
[40] Z. Li, N. Pucher, K. Cicha, J. Torgersen, S.C. Ligon, A. Ajami, W. Husinsky, A. Rosspeintner, E. Vauthey, S. Naumov, T. Scherzer, J. Stampfl, R. Liska, Straightforward synthesis and structure- activity relationship of highly efficient initiators for two- photon polymerization, Macromolecules 46 (2) (2013) 352–361.
[41] J.R. Dimmock, M.P. Padmanilayam, R.N. Puthucode, A.J. Nazarali, N.L. Motaganahalli, G.A. Zello, J.W. Quail, E.O. Oloo, H.-B. Kraatz, J.S. Prisciak, T.M. AllenCheryl, L. Santos, J. Balzarini, E. De Clercq, E.K. Manavathu, A conformational and structure- activity relationship study of cytotoxic 3,5-bis(arylidene) - 4- piperidones and related N- acryloyl analogues, J. Med. Chem. 44 (4) (2001) 586–593.
[42] H.N. Pati, U. Das, S. Das, B. Bandy, E. De Clercq, J. Balzarini, M. Kawase, H. Sakagami, J.W. Quail, J.P. Stables, J.R. Dimmock, The cytotoxic properties and preferential toxicity to tumour cells displayed by some 2, 4- bis(benzylidene) - 8- methyl- 8- azabicyclo[3.2.1]octan- 3- ones and 3, 5- bis(benzylidene) - 1- methyl- 4- piperidones, Eur. J. Med. Chem. 44 (1) (2009) 54–62.
[43] M.V. Makarov, I.L. Odinets, K.A. Lyssenko, E.Y. Rybalkina, I.V. Kosilkin, M.Y. Antipin, T.V. Timofeeva, N-Alkylated 3,5-bis(arylidene)-4-piperidones. Synthetic approaches, X-ray structure and anticancer activity, J. Heterocycl. Chem. 45 (2008) 729–736.